Optics Communications 282 (2009) 2367–2379

Contents lists available at ScienceDirect

Optics Communications

journal homepage: www.elsevier.com/locate/optcom

Bifurcations and chaos in a semiconductor laser with coherent or noisy optical injection

Sebastian Wieczorek [a,*], Weng W. Chow [b,c]

[a] Mathematics Research Institute, University of Exeter, Harrison Building, Room 325, North Park Road, Exeter EX4 4QF, UK
[b] Sandia National Laboratories, Albuquerque, New Mexico 87185-1086, USA
[c] Physics Dept. and Institute of Quantum Studies, Texas A&M University, College Station, Texas 77843, USA

ARTICLE INFO

Article history:
Received 25 November 2008
Received in revised form 19 February 2009
Accepted 22 February 2009

ABSTRACT

This paper investigates theoretically the dynamical sensitivity of semiconductor lasers to external optical signals. Bifurcation analysis of ordinary rate equations, describing noise-free lasers with pure coherent external signal, reveals that considerable modifications to the extend and type of externally induced bifurcations and chaos are possible by tailoring of the laser active-medium and resonator configurations. Extending the analysis to stochastic rate equations, which describe lasers with spontaneous emission noise and noisy external signal, reveals further dynamical effects owing to the introduced random fluctuations. In particular, phase-fluctuations (incoherence) in the external signal can have a dramatic impact on induced bifurcations and chaos. The observed strong sensitivity of laser instabilities to the intensity and coherence of external signal can provide a very sensitive means to detect ultra low levels of laser radiation.

1. Introduction

Nonlinear dynamics of laser systems is a lively field whose focus in the last two decades has been on understanding instabilities in the widely-used semiconductor lasers. A typical unperturbed semiconductor laser is a nonlinear oscillator capable of damped periodic oscillation (relaxation oscillation) or stationary-state (continuous-wave) operation. However, that may change drastically when the laser is coupled to other lasers or subjected to an external stimulus, such as optical injection or external optical feedback. In this case, the laser can undergo a number of bifurcations leading to periodic, quasiperiodic, and chaotic oscillations. This work expands on existing bifurcation studies of lasers with pure coherent optical injection, and contributes to the more general problem of instabilities in nonlinear laser oscillators driven by noisy (partially coherent) external signals [1].

Much research has been devoted to studying bifurcations and ensuing complicated dynamics in lasers with external perturbations (see for example [2–4] and references therein). It has been established that the laser response to an external optical signal strongly depends on the linewidth enhancement factor α [5–9], which quantifies the active-medium refractive index dependence on carrier population, and provides a strong nonlinear coupling between the phase and amplitude of the laser signal. Also, the limit of high quality cavity (class-A lasers) where the photon decay rate is much smaller than the polarization and carrier population decay rates was considered in Ref. [10]. However, little is understood about the dependence of the bifurcation diagram for an injected semiconductor (class-B) laser on parameters other than α. On the one hand, it was suggested that quantities such as photon and carrier decay rates, differential gain coefficient, and lasing mode confinement factor do not typically cause dramatic qualitative dynamical changes in the semiconductor laser response [7,8]. On the other hand, it was reported that coupled-semiconductor-laser dynamics strongly depends on the ratio between the carrier and photon decay rates [9]. Here, we discover and explain the strong sensitivity of externally induced bifurcations and chaos on laser parameters different than the linewidth enhancement factor.

Furthermore, previous studies of laser bifurcations and chaos are mostly focused on effects of noise-free external signals. Consequently, little is known of the effects of random fluctuations (incoherence) in the external signal [11–13], e.g. the dependence of laser dynamics on the strength of external signal noise. We address in this paper whether a highly incoherent external signal can cause locking as well as bifurcations and chaos different from those caused by pure coherent external signal. We report on first systematic study encompassing bifurcation diagrams, frequency spectra, and Lyapunov exponents to quantify noise effects on the full range of externally induced laser dynamics. In particular, we uncover and explain the strong sensitivity of locking and chaos on the strength of the external signal phase-fluctuations.

* Corresponding author.
E-mail addresses: s.m.wieczorek@ex.ac.uk, S.M.Wieczorek@exeter.ac.uk (S. Wieczorek).

0030-4018/$ - see front matter © 2009 Elsevier B.V. All rights reserved.
doi:10.1016/j.optcom.2009.02.060

Our studies are motivated by both, fundamental interest and applications of laser instabilities and chaos for remote detection of weak coherent-optical signals [14–17]. For such an application, two issues have to be addressed. The first concerns a comprehensive insight into all the physical and dynamical parameters that determine a laser sensitivity to external optical signals. The other issue concerns the effects of noise within the laser and in the external signal on the induced bifurcations and chaos. This is relevant for a realistic description of laser nonlinear behaviour in a weakly stable regime and for the determination of the laser ability to discriminate between coherent and incoherent external signals.

The laser model used in the investigation is described in Section 2. Section 3 reviews the bifurcation study of deterministic laser equations with a coherent external signal. In particular, we show that externally induced bifurcations and chaos can be significantly modified with active-medium and laser resonator design. We also provide a physical explanation of the observed dynamical sensitivity of lasers. Analysis of stochastic laser equations is performed in Section 4 to reveal the strong impact of spontaneous emission noise and external signal noise. In particular, we calculate Lyapunov exponents to identify parameter regions where noise causes significant changes to externally induced dynamics.

2. The rate equation model

We consider a single-mode semiconductor laser that receives an optical plane wave signal incident on one of its mirrors. In the framework of semiclassical laser theory, assuming quasiequilibrium condition and an active-medium polarization that adiabatically follows the time variations of the laser field and carrier population (class-B lasers [18,4]), the normalised equations of motion describing the system dynamics are [19–21]

$$\frac{dE_n}{dt} = i2\pi\Delta_n E_n + \beta\gamma(1-i\alpha)N_nE_n + f_E(t) + K|1+\kappa(t)|e^{-i\phi_i(t)}, \tag{1}$$

$$\frac{dN_n}{dt} = \Lambda_n - (N_n+1) - (1+\beta N_n)|E_n|^2 + f_N(t), \tag{2}$$

$$\frac{d\kappa}{dt} = \tau_c^{-1}\gamma_N^{-1}[-\kappa + f_\kappa(t)], \tag{3}$$

$$\frac{d\phi_i}{dt} = f_\phi(t). \tag{4}$$

The normalised complex-valued intracavity laser field E_n (henceforth, called the laser signal) is written in the units of a free-running laser field at twice threshold and reference frame of the external signal central frequency ν_i, N_n is the normalised total carrier density, and time t is in units of the carrier lifetime. $\kappa(t)$ and $\phi_i(t)$ describe fluctuations in the amplitude and phase of the injected signal, respectively. α is the linewidth enhancement factor and the normalized parameters including normalised injection strength K, detuning Δ_n, pump rate Λ_n, decay rate γ, and gain coefficient β are defined as

$$K = \frac{c\sqrt{T}|E_i|}{2n_bL\gamma_N\sqrt{1-T}|E_0|}, \quad \Delta_n = \frac{\Delta}{\gamma_N}, \quad \gamma = \frac{\gamma_c}{2\gamma_N}, \quad \Lambda_n = \frac{\Lambda}{\gamma_N N_{th}},$$
$$\beta = 1 + \frac{2c\Gamma\xi N_{tr}}{n_b\gamma_c}.$$

where Γ is the confinement factor, N_{tr} is the transparency carrier density, ξ is the differential gain at threshold carrier density $N_{th} = N_{tr} + n_b\gamma_c/(2c\Gamma)$, Λ is the carrier pump rate, γ_c and γ_N are the photon and carrier population decay rates, respectively, c is the speed of light in vacuum, n_b is the background refractive index, and Δ is the difference between injected and free-running laser central frequencies in GHz. Furthermore, the driving term K depends on the external signal amplitude $|E_i|$ as well as the optical-resonator parameters through the optical-resonator length L and the power-transmission T of the laser mirror through which the light is injected. The parameter values are given in Table 1. To relate our calculations to laser experiments we use

$$\text{injection intensity } (\mathrm{W/m^2}) = \frac{1}{2}c\epsilon_0|E_i|^2 = \frac{4\hbar\nu L^2\Gamma N_{th}\gamma_N^3(1-T)}{c\gamma_c T}K^2.$$

Noise is represented by the random functions [20,24] $f_a(t)$ that are Gaussian, have zero mean, and are delta correlated

$$\langle f_a(t)f_a(t')\rangle = 2D_a\delta(t-t'), \tag{5}$$
$$\langle f_a(t)\rangle = 0, \tag{6}$$

where $a = E,N,\kappa,\phi$. Spontaneous emission and non-radiative recombinations in the laser are described by $f_E(t) = f_E'(t) + if_E''(t)$ and $f_N(t)$ with diffusion coefficients

$$2D_E = \frac{C_{sp}\gamma}{\Gamma},$$
$$2D_N = \left(\frac{C_{sp}\Gamma}{\gamma}|E_n|^2 + \frac{2}{N_{th}V}\right),$$

chosen to be consistent with the coefficients for the fluctuations in the photon number, optical phase, and carrier number, respectively, as derived by Henry [24]. The model allows for amplitude- and phase-fluctuating external signal through the time-dependent $\kappa(t)$ and $\phi_i(t)$. The amplitude noise $\kappa(t)$ of the external-field is exponentially correlated with zero mean, variance $\tau_c^{-1}D_\kappa$ and correlation time τ_c [Eq. (3)]. The phase of the external-field $\phi_i(t)$ is a random variable [Eq. (4)] so that the resulting frequency spectrum of an external signal with just phase-fluctuation has a Lorentzian lineshape with a linewidth (full width at half maximum) of D_ϕ/π as shown in [25,11] and also verified in our case. Such description of the external signal fluctuations is consistent with the effects of spontaneous emission inside the cavity of an external (master) laser.

Eqs. (1) and (2) assume single-mode operation, which is consistent with typical vertical cavity emitting lasers (VCSELs) and specialised edge emitters with coated facets or distributed Bragg reflectors (DBR). In distributed feedback (DFB) lasers, the definition of the round-trip time, transmission parameter T, and the feed-in rate $c/(2n_bL\sqrt{1-T})$ is less straightforward due to the distributed reflection added to the facet reflections. In particular, the grating parameters have to be taken into account in deriving the feed-in rate and the model used here may not be applicable [26].

3. Sensitivity to coherent external signals

This section investigates solutions to Eqs. (1) and (2) with $D_E = D_N = D_\kappa = D_\phi = 0$, to further understand the response of a

Table 1
Parameters for the unperturbed lasers.

Parameter	Symbol	Laser A	Laser B
Transparency carrier-density	N_{tr} ($\mathrm{m^{-3}}$)	2×10^{24}	2×10^{24}
Differential gain coefficient	ξ ($\mathrm{m^2}$)	10^{-19}	10^{-19}
Background refractive index	n_b	3.4	3.4
Linewidth enhancement factor	α	4	4
Confinement factor	γ	0.05	0.05
Carrier decay rate	γ_N ($\mathrm{s^{-1}}$)	10^9	2×10^9
Photon (cavity) decay rate	γ_c ($\mathrm{s^{-1}}$)	10^{12}	10^{11}
Laser wavelength	λ (μm)	1	1
Cavity length	L (μm)	0.3	200
Mirror transmission	T	0.001	0.2
Spontaneous emission coefficient	C_{sp}	2×10^{-5}	2×10^{-5}
Active volume	V ($\mathrm{m^{-3}}$)	10^{-17}	10^{-18}

noise-free laser to a coherent (single-frequency) external signal. As the parameters are varied, one finds qualitative changes in the solutions, i.e. bifurcations, of Eqs. (1) and (2). Bifurcation curves were calculated in the two-dimensional plane of external signal intensity and detuning using the bifurcation continuation software AUTO [27]. The resulting bifurcation diagram divides the two-dimensional plane of external signal intensity and frequency detuning into regions of qualitatively different dynamics and contains the information on dynamical sensitivity of the laser. Such bifurcation diagrams have been intensively studied and their dependence on the linewidth enhancement factor is well understood: α causes the asymmetry in the bifurcation diagram and increases the number of instabilities [6,9]. Also, theoretical bifurcation diagrams show remarkably good agreement with laser experiments [28–31]. This section reports on significantly different response of two lasers which have identical α but different active-medium and optical-resonator parameters. These results are explained by examining the relaxation oscillation frequency and damping rate in an unperturbed laser.

3.1. Effects of active-medium and optical-resonator

Here, we consider two different lasers, A and B, whose parameters are specified in Table 1. Their population decay rates differ by a factor of 2, and different optical-resonator parameters (T and L) result in a factor of 10 difference in their photon decay rate. The other parameters, including α and the pump rate Λ, are identical for both lasers.

Fig. 1 shows bifurcation diagrams in the plane of external signal intensity and frequency detuning for lasers A and B. A stable equilibrium of deterministic (with noise terms set to zero) Eqs. (1) and (2) corresponds to optical-phase locking of the laser signal to the external signal. The stable equilibrium exists in the shaded region bounded by the supercritical branches of saddle-node S and Hopf H bifurcation curves which become tangent at the saddle-node-Hopf point G. Outside the shaded region one finds interesting solutions to Eqs. (1) and (2) such as periodic orbits of various periods, quasiperiodic tori, and chaotic attractors, which all correspond to oscillating laser intensity [4]. In particular, laser intensity oscillations are periodic of frequency Δ near $K = 0$. With increasing K, a number of instabilities and complicated nonlinear dynamics appear before locking is reached at either Hopf H or saddle-node S bifurcation. Detailed bifurcation structures leading to complicated dynamics and chaos are discussed in Ref. [4]. Here, we plot only period-doubling bifurcation curves PD. They indicate a typical instability of a periodic orbit of basic period and provide a good indication of regions with complicated dynamics in this system.

The two bifurcation diagrams in Fig. 1 show fairly similar frequency extent of externally induced instabilities but differ in two significant aspects. One aspect is the striking difference in the external signal intensity required to trigger instabilities. Instabilities in laser A are triggered by an external signal whose intensity is almost 10^6 times lower than the intensity required to trigger instabilities in laser B. Also, laser A requires less intense external signal to achieve locking over a wide range of frequency detuning. The other aspect is the striking difference in the type of dynamics induced by the external signal. Regions of complicated dynamics in the plane of injection intensity and detuning are much smaller for laser B. Furthermore, laser B appears to have very few instabilities and no chaotic dynamics is found inside the considered period-doubling curve (Fig. 2b). In contrast, laser A undergoes a number of instabilities and shows a rich display of complicated and chaotic oscillations. This is illustrated with one-dimensional bifurcation diagrams in Fig. 2 where we plot maxima of the (oscillating) laser intensity versus the external signal intensity for fixed detuning. Note that periodic orbit of a basic period has one maximum, and periodic orbit of twice the basic period born in the period-doubling bifurcation has two maxima. Subsequent splittings in Fig. 2a correspond to subsequent period-doublings leading to chaotic oscillations whose amplitude increases abruptly, up to 10 times the unperturbed laser intensity, at $\approx 0.1\,\mathrm{W/cm^2}$. Clearly, laser A shows more complicated dynamics and much stronger intensity oscillations than laser B despite the fact that it receives $\approx 10^5$ times less intense external signal of similar frequency.

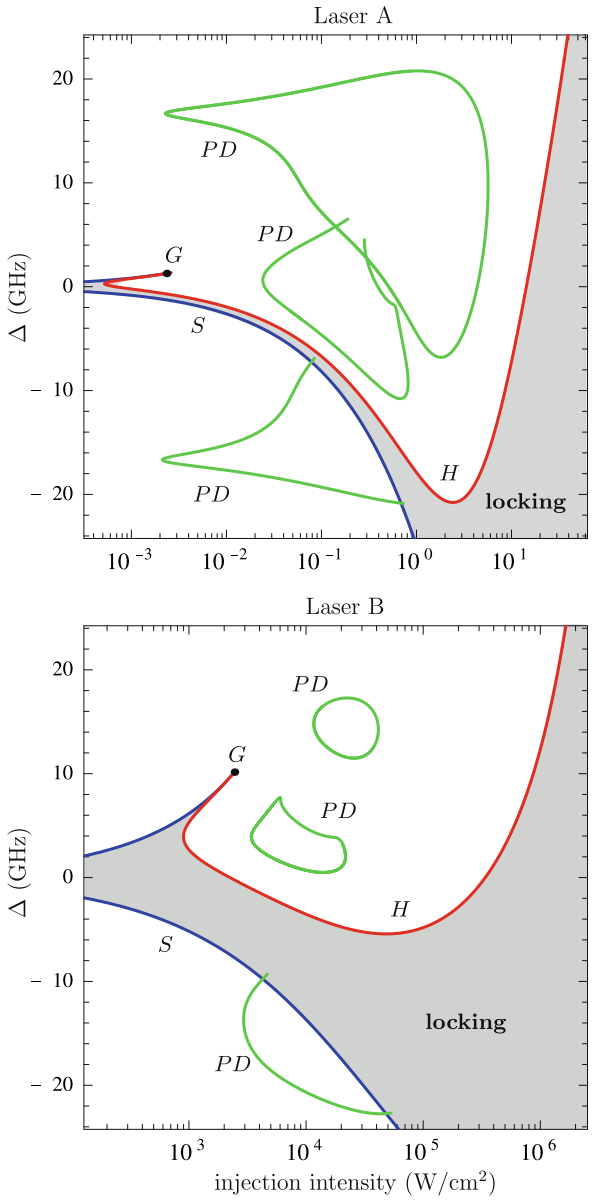

Fig. 1. Two-dimensional bifurcation diagram in the plane of the external signal intensity and frequency detuning for injected lasers (top) A and (bottom) B. Both lasers have the same $\alpha = 4$ and are pumped at twice the lasing threshold $\Lambda_n = 2$; see Table 1 for other parameters.

At twice the lasing threshold, the intracavity field intensity, calculated as $\frac{1}{2}\epsilon_0 n_b c|E|^2$, in lasers A and B is $4.1 \times 10^4\,\mathrm{W/cm^2}$ and $5.6 \times 10^5\,\mathrm{W/cm^2}$, respectively. In the case of laser A (B), this is approximately $10^7(10^2)$ times more than the intensity of the external field required to trigger period-doubling bifurcation. Because of the richer dynamics and our interest in dynamics-based coherent-signal detection, we focus henceforth on the response of laser A.

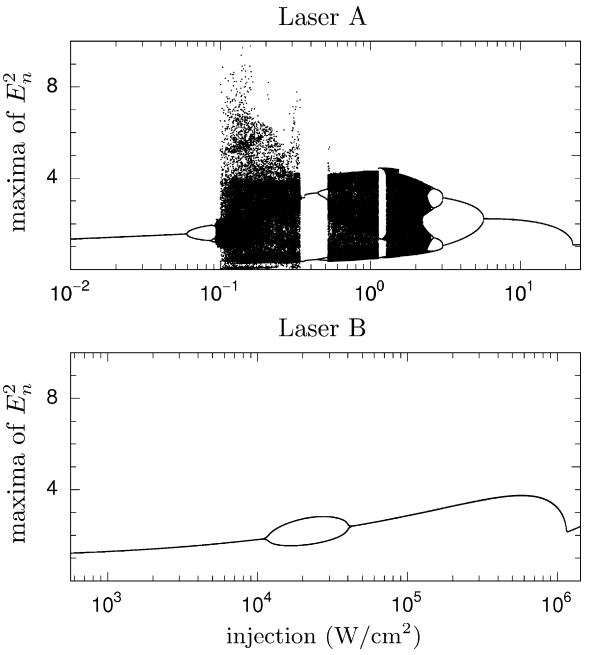

Fig. 2. One-dimensional bifurcation diagram shown as maxima of the (oscillating) laser output E_n^2 plotted vs. the external signal intensity for injected lasers (top) A and (bottom) B. $\Lambda_n = 2$ and $\Delta =$ (top) 10 GHz and (bottom) 15 GHz.

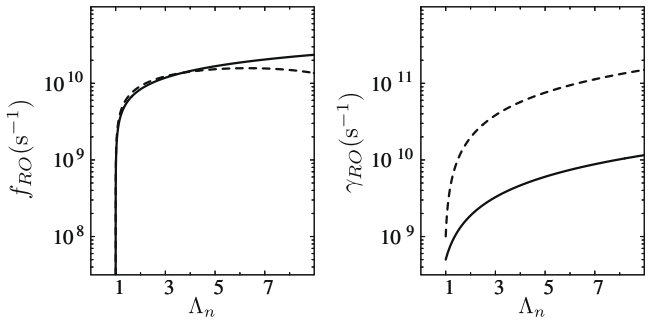

Fig. 3. (Left) Relaxation oscillation frequency and (right) damping rate vs. the normalized pump rate in the unperturbed lasers (solid curves) A and (dashed curves) B.

3.2. Physical explanation

This section identifies the physical and dynamical mechanisms underlying drastically different sensitivity of lasers A and B to an external optical signal.

Let us recall that the simple damped oscillatory dynamics of an unperturbed laser can be characterized by its relaxation oscillation (RO) frequency and damping rate:

$$f_{RO}^{fr} = \frac{1}{2\pi}\sqrt{2\gamma_{RO}^{fr}\gamma_c - \gamma_N\gamma_c - (\gamma_{RO}^{fr})^2}, \tag{7}$$

$$\gamma_{RO}^{fr} = \frac{c\Gamma^{\xi}}{n_b\gamma_c}(\Lambda - \gamma_N N_{tr}), \tag{8}$$

From a nonlinear dynamics point of view, γ_{RO}^{fr} quantifies the stability and f_{RO}^{fr} is the characteristic frequency of a damped nonlinear laser oscillator. These two quantities give some insight into nonlinear response of a perturbed laser. On the one hand, the RO frequency quantifies a frequency detuning range within which nonlinear resonances and associated instabilities arise in response to external signals. Specifically, asymptotic bifurcation analysis showed that the two period-doubling bifurcation curves, roughly indicating the frequency extent of externally induced instabilities, originate near $K = 0$ at frequencies $\pm 2f_{RO}$, respectively [33]. This analytical result agrees well with numerical bifurcation analysis of the full model and shows that the frequency extent of externally induced instabilities is approximately four times the RO frequency of the unperturbed laser. On the other hand, RO damping rate quantifies the rate of external perturbation required for transition to sustained oscillation. Such a transition is a first step towards complicated and chaotic dynamics and can be thought of as externally induced decrease to zero in the otherwise positive RO damping rate. Consequently, external signal intensity required to trigger instabilities, as well as the overall dynamical response of the laser, are both expected to strongly depend on the RO damping rate of the unperturbed laser.

Fig. 3 shows that, for a realistic choice of active-medium and optical-resonator parameters, two equally pumped semiconductor lasers can have similar RO frequency but significantly different RO damping rate (Fig. 3). Indeed, the drastic differences in the type of instabilities induced by an external coherent signal in lasers A and B (shown in Figs. 1 and 2) arise from the 10-fold difference in the RO damping rate of the two unperturbed lasers. Furthermore, the appreciable difference in the external signal intensity required to destabilise the laser arises from two sources. One source is the difference in γ_{RO}^{fr} and accounts for the difference of $\sim 10^2$ in the external signal intensity from diagrams in Fig. 1. The other source is the difference in the parameters of the optical-resonator. The driving term in Eq. (1) includes the coupling coefficient $c\sqrt{T}/(2n_bL\sqrt{1-T})$ which quantifies the rate at which the fraction of the external signal that makes it through the mirror adds the circulating intracavity laser signal. To effectively couple an external signal into the optical-resonator, one requires a high $c\sqrt{T}/(2n_bL\sqrt{1-T})$. We find that the difference in optical-resonators is responsible for the remaining $\sim 10^3$ difference in the external signal intensity found in diagrams in Fig. 1.

The RO frequency and damping rate, being the real and imaginary parts of a complex root of a quadratic polynomial, are intrinsically linked [Eqs. (7) and (8)]. With γ_{RO} being a linear function of Λ, any increase in the RO frequency is associated with a corresponding increase in the RO damping rate. This link causes the trade-off between sensitivity and bandwidth of externally induced instabilities.

4. Sensitivity to noise

The bifurcation analysis used to investigate the ordinary differential equations describing noise-free lasers with coherent-signal injection is not applicable for studying the stochastic differential equations describing noisy lasers with noisy signal injection. The problem lies in the description of dynamics and definition of a bifurcation, that is a change in the type of dynamics, in the presence of noise [37]. The possibilities include temporal characteristics of dynamical variables, frequency spectra, Lyapunov exponents of corresponding attractors, and probability densities for trajectories in phase space. Therefore, it is important to clearly identify what is meant by an instability in a random dynamical system such as a noisy laser. In the theory of random dynamical systems, one speaks of a random sink when the largest Lyapunov exponent is negative and of a random strange attractor when the largest Lyapunov exponent is positive. In a laser experiment or computer simulation, these two types of a random attractor can be difficult to distinguish from direct observations as they may lead to similar erratic time series with broad and non-discrete frequency spectra. However, they differ in at least one aspect, that is sensitivity on initial conditions which is quantified by Lyapunov exponents. For the purpose of our work, it is satisfactory to study

Lyapunov exponents of random attractors and define an instability as a passing of a Lyapunov exponent through zero.

In the next two sections, we focus on a particular bifurcation transition for fixed Δ and varying external signal intensity. This transition is illustrated with the frequency spectra of the laser signal, one-dimensional bifurcation diagrams showing maxima of the (oscillating) laser intensity, and Lyapunov exponents of the corresponding random attractors. Such a choice allows comparison of information which is typically obtained from a semiconductor laser experiment (frequency spectra), a direct numerical time integration (time series), and information on the type of dynamics, e.g. chaotic or non-chaotic (Lyapunov exponents). Recall that a Lyapunov exponent is an exponential rate at which different trajectories, starting at infinitesimally close initial conditions, approach (negative Lyapunov exponent) or separate (positive Lyapunov exponent) from each other. A positive Lyapunov exponent quantifies sensitivity on initial conditions (unpredictability) and amount of chaos. The three-dimensional laser system has three or less distinct Lyapunov exponents. In a noise-free laser, a stable equilibrium has three negative Lyapunov exponents, a stable periodic orbit has two negative and one zero Lyapunov exponent, a stable quasiperiodic torus has one negative and two zero Lyapunov exponents, and a chaotic attractor has one negative, one zero, and one positive Lyapunov exponent. Locking to a noise-free external signal is represented by a stable equilibrium meaning that the laser oscillation follow the external signal. In a noisy laser, one finds either random sink with three negative Lyapunov exponents or random strange attractor with one positive and two negative Lyapunov exponents. Locking to a noisy external signal is represented by a random sink. However, it is different from the noise-free locking. Namely, it may be impossible to see wheather the laser follows the noisy external signal owing to a complicated, relationship between the noisy external signal and the locked laser signal. In fact, locking (or synchronisation) to a noisy external signal manifests as a reproducible response to the same noisy external signal applied repeatedly to the laser at different initial conditions (or, alternatively, identical response of two or more uncoupled lasers driven by the same noisy external signal) [1]. We denote the three Lyapunov exponents in decreasing order as l_1,l_2 and l_3. The largest Lyapunov exponent can be calculated from noisy time series [38,39] and it should be possible to experimentally verify all the phenomena uncovered in this section.

4.1. Effects of spontaneous emission noise

This section investigates solutions to stochastic Eqs. (1) and (2) with $D_E \neq 0$,$D_N \neq 0$ and $D_\kappa = D_\phi = 0$, to determine the effect of spontaneous emission noise on the injection-induced instabilities in the weakly-stable laser A, studied in Section 3. The study expands on previous studies of spontaneous emission noise effects [35] by identifying parameter regions where spontaneous emission noise causes significant deviations from nonlinear dynamics of the noise-free laser.

We show in Fig. 4, for different pump rates $\Lambda_n = 1.2$, 2, and 6, that a substantial spontaneous emission noise effect can be seen already in the frequency spectra of unperturbed lasers (all spectra are referenced to the unperturbed laser frequency). In the spectra, the large central peak corresponds to the lasing mode and the smaller side peaks correspond to noise-excited RO and its higher harmonics. Notice that the weakly stable laser A exhibits non-harmonic RO and requires a much stronger pump rate to develop a noticeable lasing mode. Noise effects on bifurcations and chaotic dynamics of the injected laser A at different pump rates Λ_n are depicted in pairs of Figs. 5–10, respectively.

We first focus on frequency spectra in Figs. 5, 7, and 9, and one-dimensional bifurcation diagrams in Figs. 6, 8, and 10. Bifurcation

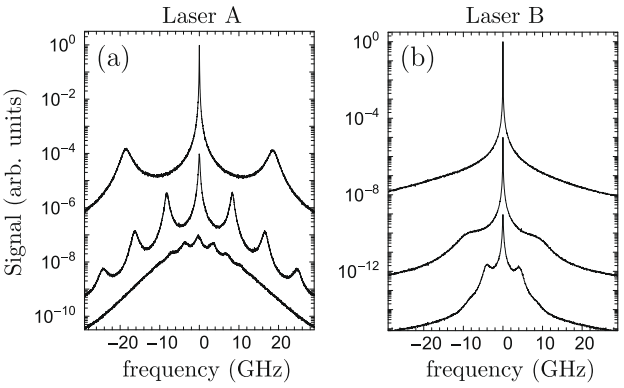

Fig. 4. Frequency spectra of unperturbed lasers (a) A and (b) B with spontaneous emission noise. $C_{sp} = 2 \times 10^{-5}$ and the normalized pump rate Λ_n=(bottom) 1.2, (middle) 2, and (top) 6. The spectra were shifted along the y-axis for clarity.

diagrams of a noise-free laser from the top panel of Figs. 6, 8, and 10 show similar bifurcation scenario for all three settings of Λ_n. Dynamics at seven particular values of the external signal intensity are illustrated with frequency spectra in Figs. 5, 7, and 9. For external signal intensities below the instability threshold, the noise-free spectra from the left column in Figs. 5, 7, and 9 consist of a peak at the injection-modified lasing-mode frequency, the peak at the external signal frequency Δ, and its (complex conjugate) counterpart at $-\Delta$ due to nonlinear wave mixing process [34] [Figs. 5a1, 7a1 and b1, and 9a1 and b1]. As the external signal intensity increases, the laser undergoes period-doubling bifurcation which is accompanied by the appearance of additional peaks at half-way between the already existing peaks [Figs. 5b1, 7c1, and 9c1]. Subsequent bifurcations lead to chaotic dynamics which manifests as a continuum of frequencies with no distinct periodic components (except for the external signal component at Δ) in the frequency spectrum [Figs. 5c1, 7d1, and 9d1]. Next, inverse period-doubling bifurcations lead to period-two oscillation [Figs. 5d1, 7e1, and 9e1] and then to period-one oscillation [Figs. 5e1, 7f1, and 9f1]. With further increase in the external signal intensity, phase locking is achieved via Hopf bifurcation [Figs. 5f1, 7g1, and 9g1].

Spectra from the right column in Figs. 5, 7, and 9, show effects of spontaneous emission noise. It is clear from Figs. 5 and 6a and b that for $\Lambda_n = 1.2$ spontaneous emission noise "washes out" bifurcations found in the noise-free laser. Hardly any bifurcation identified from the noise-free spectra in the left column in Fig. 5 can be concluded from the noisy spectra in the right column. Similarly, there is no resemblance between the two bifurcation diagrams in Fig. 6a and b. Conclusive results on the level of the noisy spectra start to appear for $\Lambda_n = 2$ (Fig. 7). Around this value of Λ_n, noisy bifurcation diagram starts to resemble deterministic bifurcation diagram [Fig. 8a and b]. In particular, at low external signal intensities, nonlinear intracavity wave mixing [Fig. 7a2 and b2] can be distinguished, and the subsequent period-doubling bifurcation starts to be visible [Fig. 7b2 and c2]. Spontaneous emission noise makes significantly less impact at higher pump rates as is shown in Figs. 9 and 10 for $\Lambda_n = 6$. There, each bifurcation identified in the left column of Fig. 9 can be concluded from the noisy spectra in the right column. Similarly, the noisy and deterministic bifurcation diagrams show close resemblance (Fig. 10). Finally, we note that noisy spectra in Figs. 7 and 9 have elements that are absent in the corresponding spectra of the deterministic system. These elements include excitation of otherwise damped resonances such as RO [panels (a2) and (g2)], nonlinear wave mixing processes [panels (b2)], and anticipation of imminent bifurcations [panels (b2) and (f2)].

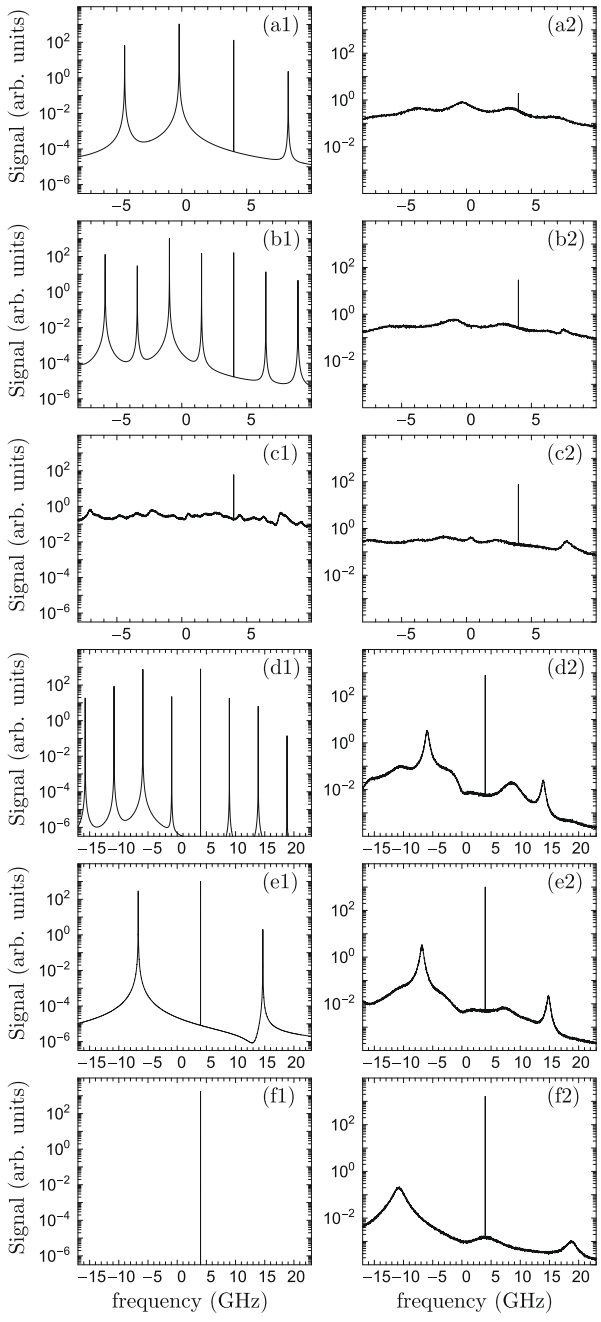

Fig. 5. Bifurcation transition in Laser A injected with a coherent signal shown as frequency spectra of the laser signal (left column) without and (right column) with spontaneous emission noise. $\Lambda_n = 1.2, \Delta = 4$ GHz, $C_{sp} = 2 \times 10^{-5}$, and from top to bottom the external signal intensity in units of W/cm^2 = 0.000156, 0.003, 0.01, 0.181, 0.3, and 1.0.(K = 0.5, 2.2, 4, 17, 22, and 40).

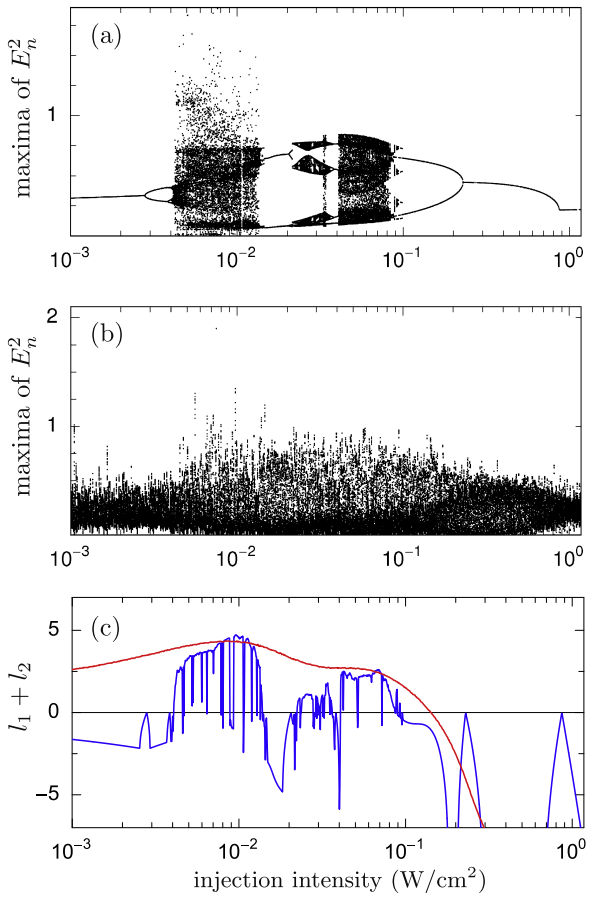

Fig. 6. (Top two panels) One-dimensional bifurcation diagram of an injected laser A plotted as maxima of the (oscillating) laser intensity E_n^2 vs. the external signal intensity (a) without and (b) with spontaneous emission noise. Panel (c) shows the sum of two largest Lyapunov exponents (lower curve, blue) without and (upper curve, red) with spontaneous emission noise. $\Lambda_n = 1.2$, $\Delta = 4$ GHz and $C_{sp} = 2 \times 10^{-5}$.

With spontaneous emission noise, the frequency spectra and bifurcation diagrams can indicate the type of dynamics observed well above the lasing threshold ($\Lambda = 6$) but are completely inconclusive near the lasing threshold ($\Lambda = 1.2$). Consequently, interesting questions arise about some erratic oscillations observed near the lasing threshold [e.g. Fig. 6b]. Namely, are they ordinary noisy fluctuations (non chaotic random attractors) or chaos (chaotic random attractors)? The answer is obtained from calculating Lyapunov exponents plotted in blue for the noise-free laser and in red for the noisy laser in panel (c) of Figs. 6, 8, and 10. The blue curve in panel (c) of Figs. 6, 8, and 10 starts at negative values, passes through zero at bifurcation points but remains at negative values till it crosses over to positive values indicating the chaotic region with infinitely many windows of periodic dynamics. These results are in perfect agreement with the more accurate approach of bifurcation continuation from Section 3. The red curve in panel (c) of Figs. 6, 8, and 10 shows the effect of spontaneous emission noise. In general, one observes three qualitative changes in laser dynamics owing to noise: (i) disappearance of some passings through zero, (ii) disappearance of periodic windows within chaos, and (iii) expansion of the chaotic region [35,40]. Furthermore, there are significant differences for different values of the normalised pump rate. For $\Lambda_n = 1.2$, most passings through zero and all periodic windows disappear, and the chaotic region is significantly expanded, especially over the lower values of the external signal intensity. This is where periodic oscillations of the noise-free laser turn chaotic under influence of noise (noise-induced chaos). For $\Lambda_n = 2$, there is a much less expanded chaotic region and one notices signatures of largest periodic window. For $\Lambda_n = 6$, the red curve closely follows the blue curve recovering many passings through zero as well as the chaotic region with its largest periodic window. It only misses smaller periodic windows within chaos and some passings through zero at low external signal intensities. For all three settings of Λ_n, noise has a stronger effect on instabilities at lower external signal intensities.

Observed here variations in spontaneous emission noise effects can be understood intuitively. One straightforward way is to intro-

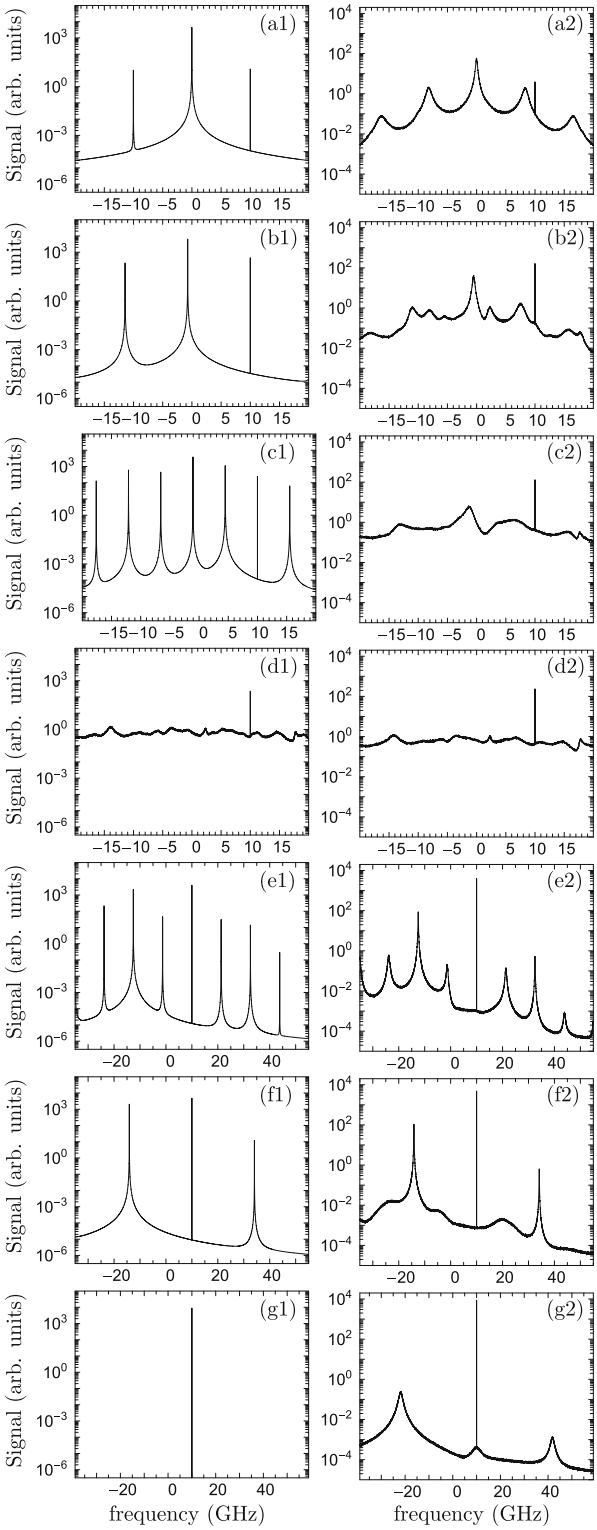

Fig. 7. Bifurcation transition in Laser A injected with a coherent signal shown as frequency spectra of the laser signal (left column) without and (right column) with spontaneous emission noise. $A_n = 2$, $\Delta = 10$ GHz, $C_{sp} = 2 \times 10^{-5}$, and from top to bottom the external signal intensity in units of W/cm^2 = 0.000156, 0.0156, 0.0756, 0.16, 5.0 and 25.0 (K = 0.5, 5.0, 11, 16, 90, 110, and 200).

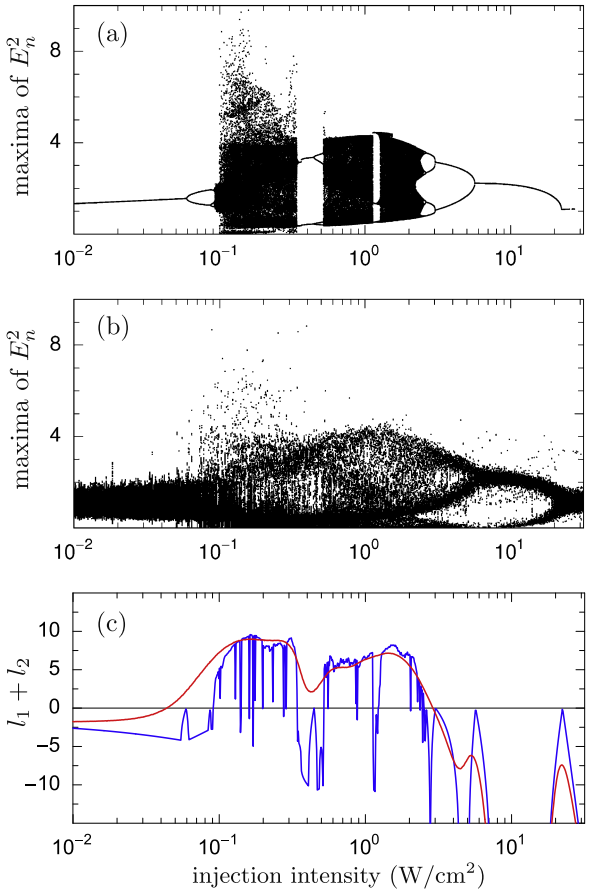

Fig. 8. (Top two panels) One-dimensional bifurcation diagram of an injected laser A shown as maxima of the (oscillating) laser output E_n^2 vs. the external signal intensity (a) without and (b) with spontaneous emission noise. Panel (c) shows the sum of two largest Lyapunov exponents (lower curve, blue) without and (upper curve, red) with spontaneous emission noise. $A_n = 2$, $\Delta = 10$ GHz and $C_{sp} = 2 \times 10^{-5}$.

duce the relative noise strength equal to γ_N/γ_{las}, where γ_N quantifies the spontaneous emission rate and γ_{las} is the characteristic decay rate or inverse timescale of the transient dynamics of the laser. While γ_N remains fixed, γ_{las} can vary significantly with the pump rate and external signal parameters, resulting in pump and perturbation dependent relative noise strength. In an unperturbed laser, $\gamma_{las} = \gamma_{RO}^{fr}$ and hence the increasing noise impact with decreasing pump rate, as well as the much stronger noise effect on the unperturbed laser A (Fig. 5). In an injected laser, the timescale of the transient dynamics can be appreciably modified from its unperturbed-laser value [21]. Under weak injection, $\gamma_{las} \approx \gamma_{RO}^{fr}$. Under strong injection, it can vary between $\gamma_{las} \ll \gamma_{RO}^{fr}$ and $\gamma_{las} \approx 100\gamma_{RO}^{fr}$. For the particular bifurcation scenario discussed here, γ_{las} increases to above γ_{RO}^{fr} with the external signal intensity. Therefore, much stronger noise effect is observed on the instabilities induced by low-intensity external signals (Figs. 5–10).

We found the effect of carrier density fluctuation to be negligible compared to photon density fluctuation, which is consistent with the results in Refs. [23,24]. While intrinsic carrier fluctuations were recognised to have a non-negligible effect in certain laser systems with delay [13], setting $f_N(t) = 0$ in Eq. (2) causes no visible changes to the results.

4.2. Effects of external signal noise

This section investigates solutions to stochastic Eqs. (1)–(4) with $D_E = D_N = 0$ and $D_\phi \neq 0$ and $D_\kappa \neq 0$ to determine the effect of the external signal fluctuations on the injection-induced instabilities in the weakly stable laser A, studied in Section 3. First, we set

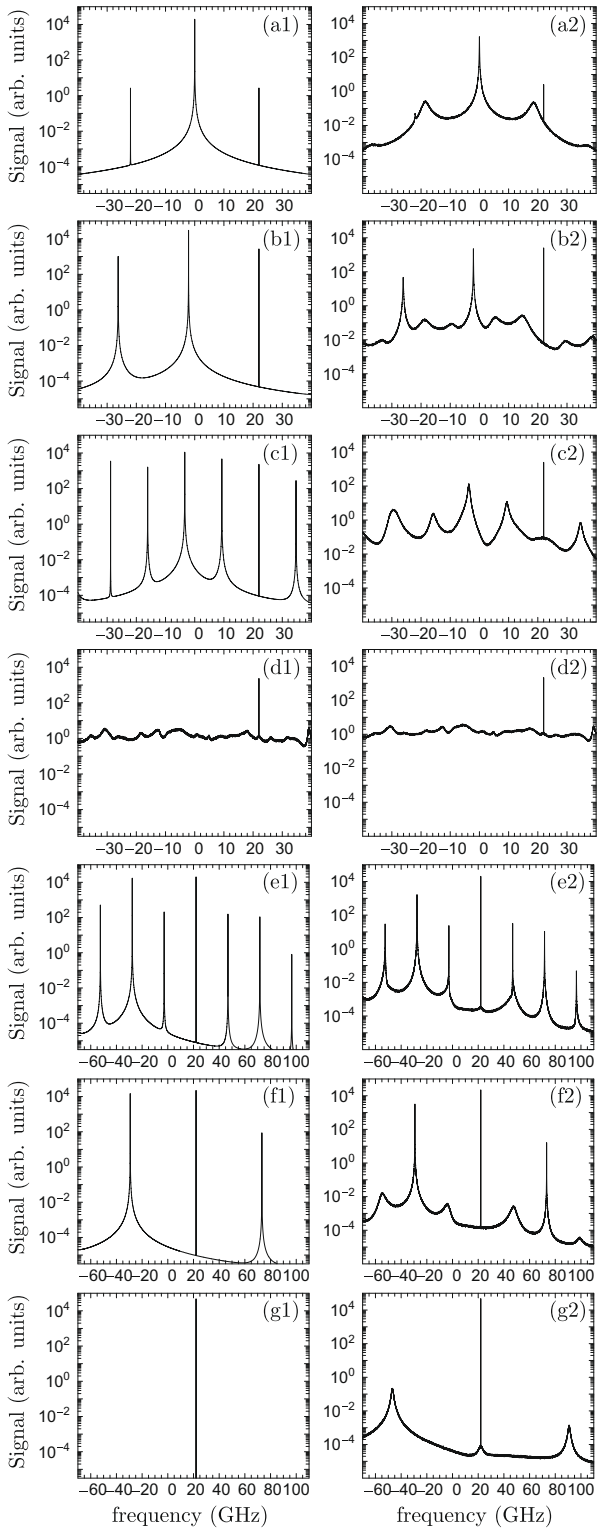

Fig. 9. Bifurcation transition in Laser A injected with a coherent optical signal shown as frequency spectra of the laser field (left column) without and (right column) with spontaneous emission noise. $\Lambda_n = 6$, $\Delta = 22$ GHz, $C_{sp} = 2 \times 10^{-5}$, and from top to bottom the external signal intensity in units of W/cm^2 = 0.000156, 0.563, 1.9, 4.0, 126.6, 156.3, and 625 ($K = 0.5$, 30, 55, 80, 450, 500, and 1000).

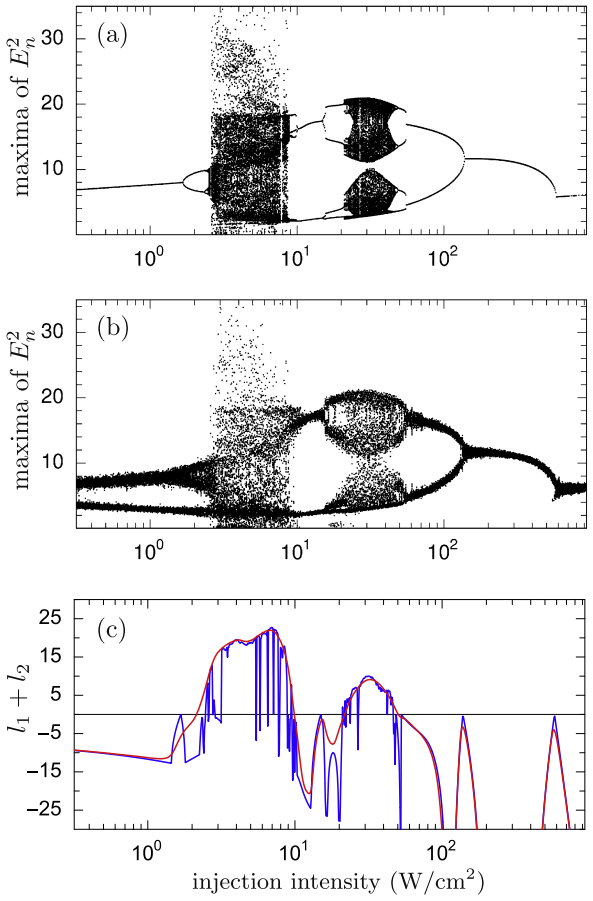

Fig. 10. (Top two panels) One-dimensional bifurcation diagram of an injected laser A shown as maxima of the (oscillating) laser output E_n^2 vs. the external signal intensity (a) without and (b) with spontaneous emission noise. Panel (c) shows the sum of two largest Lyapunov exponents (lower curve, blue) without and (upper curve, red) with spontaneous emission noise. $\Lambda_n = 6$, $\Delta = 22$ GHz and $C_{sp} = 2 \times 10^{-5}$.

$D_\kappa = 0$ and study effects of phase-fluctuations. Specifically, we consider bifurcation transition shown in Fig. 2 (a) for $D_\phi = 0$, and investigate its dependence on D_ϕ. Second, we set $D_\phi = 0$ and study effects of amplitude fluctuations for different values of the external signal correlation time τ_c. In this section we excluded spontaneous emission noise to extract effects purely due to the external signal fluctuations. Including spontaneous emission noise affects data at low injected signal intensities [e.g. panels (b1)–(b3) and (c1) in Fig. 11] as is described in Section 4.1.

4.2.1. Phase noise

The rate of the external signal phase-fluctuations D_ϕ/π gives the external signal linewidth in units of inverse second, and its inverse is the external signal coherence-time. Let us first focus on frequency spectra from Fig. 11 and one-dimensional bifurcation diagrams from the left column in Fig. 12. Bifurcation diagrams in Fig. 12 show the transition at fixed $\Delta = 10$ GHz and varying external signal intensity for different values of D_ϕ. Dynamics at seven particular values of the external signal intensity are illustrated with frequency spectra in Fig. 11, where each column corresponds to different D_ϕ. On the level of frequency spectra, all the bifurcations found for pure coherent external signal [Fig. 11a1–a7] are clearly distinguishable from frequency spectra for $D_\phi/\pi = 10^7$ s^{-1} [Fig. 11b1–b7]. In the bifurcation diagram, we observe slight smearing of bifurcation points but most bifurcations can be distinguished [Fig. 12b1]. For $D_\phi/\pi = 10^9$ s^{-1}, there are noticeable changes between the individual spectra but the bifurcations of the deterministic laser are no longer distinguishable [Fig. 11c1–c7]. Similarly, particular bifurcations in the bifurcation diagram

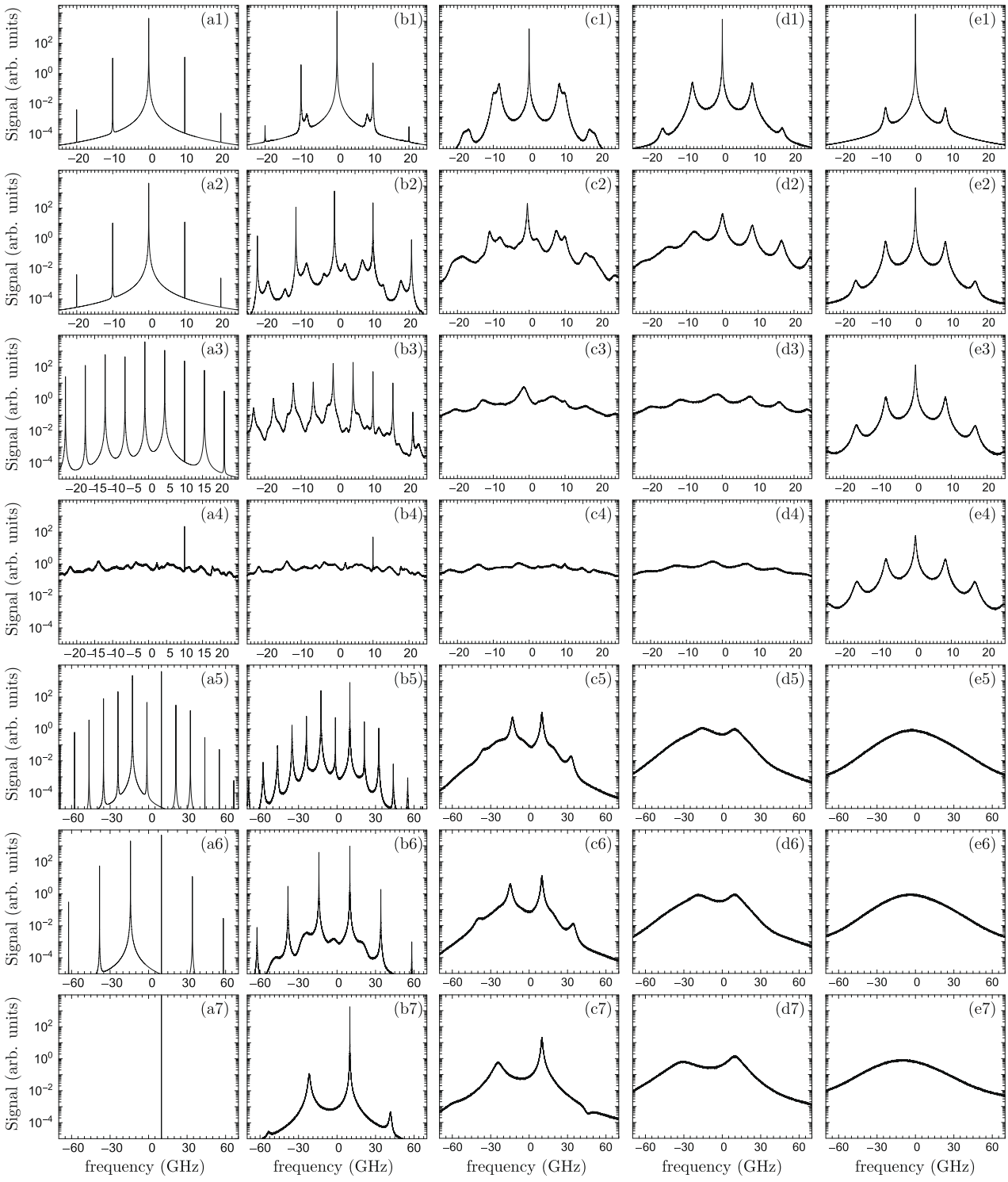

Fig. 11. Frequency spectra of Laser A injected with a noisy signal at $\Delta = 10$ GHz and $\Lambda_n = 2$. From top to bottom, the external signal intensity in units of W/cm^2 = 0.000156, 0.0156, 0.0756, 0.16, 5.0 and 25.0 ($K = 0.5$, 5.0, 11, 16, 90, 110, and 200). From (a) to (e) the rate of the external signal phase-fluctuation $D_\phi/\pi(\mathrm{s}^{-1}) = 0$, 10^7, 10^9, 10^{10}, and 10^{12}. Compare each column with the corresponding panel in Fig. 12.

in Fig. 12c1 are no longer distinguishable but some features of the response to a coherent-signal, including the large-amplitude oscillations near 0.1 W/ cm^2 of the injected power, are still present. For $D_\phi/\pi = 10^{10}\ \mathrm{s}^{-1}$, most of the features seen in frequency spectra in column (a) disappear and there is even less variation between different spectra in panels (d1)–(d7). With increasing external signal intensity, the laser spectrum evolves from what is typically observed for a noisy unperturbed laser [Fig. 11d1–d3] to a flat and wide shape with two components near the external signal and the injection-modified lasing mode frequencies, respectively [Fig. 11d5–d7]. In the bifurcation diagram [Fig. 12d1], most similarities to the noise-free injection [Fig. 12a1] have disappeared. For $D_\phi/\pi = 10^{12}\ \mathrm{s}^{-1}$, there is no resemblance to the pure coherent case whatsoever. On the one hand, a phase-fluctuating external

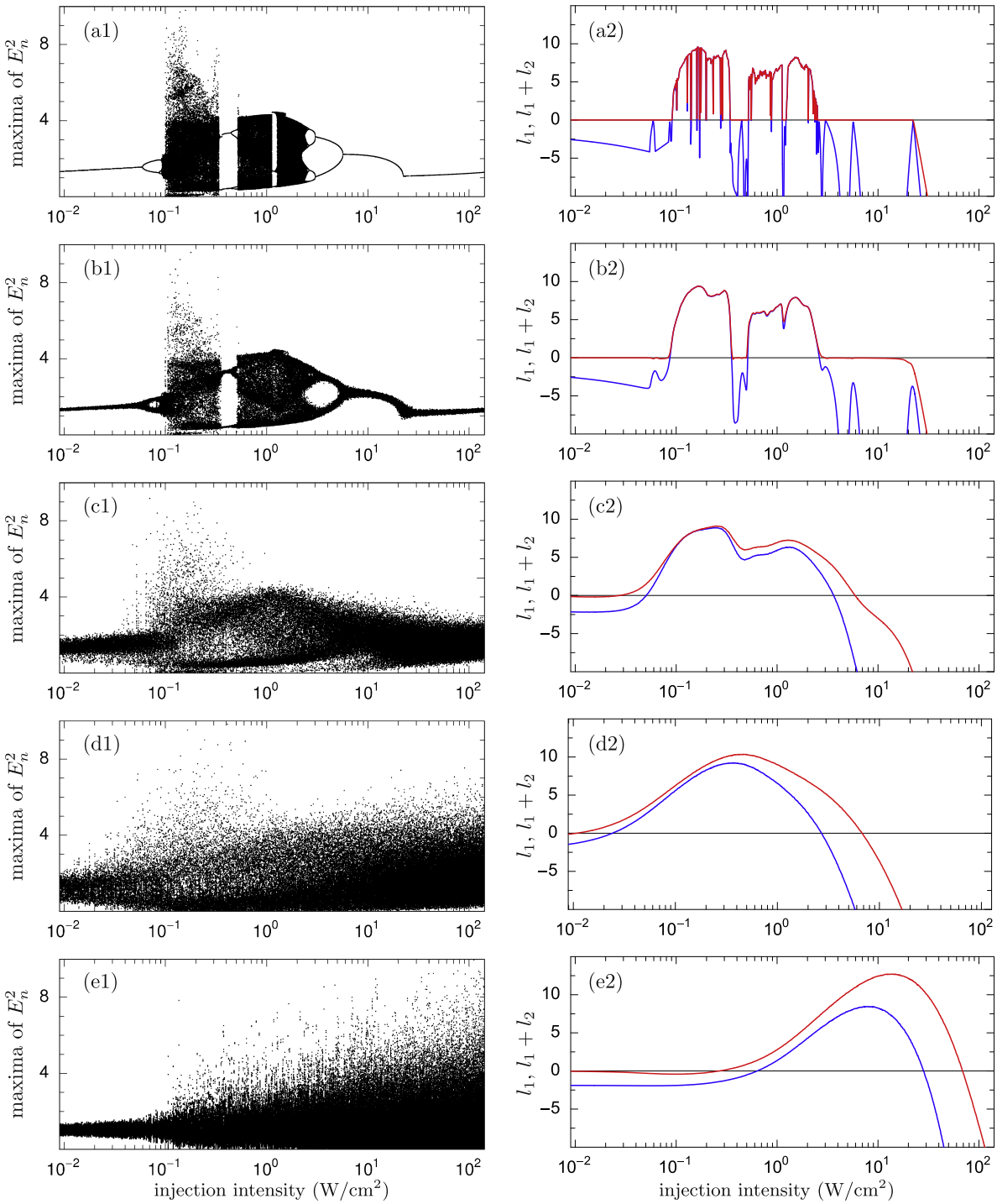

Fig. 12. (Left column) One-dimensional bifurcation diagram of an injected Laser A shown as maxima of the (oscillating) laser output E_n^2 plotted vs. the external signal intensity for $\Delta = 10$ GHz. (Right column) The largest Lyapunov exponent (upper curve, red) and the sum of two largest Lyapunov exponents (lower curve, blue) for the transition shown in the left column. From (a) to (d) the rate of the external signal phase-fluctuations $D_\phi/\pi(s^{-1}) = 0$, 10^7, 10^9, 10^{10}, and 10^{12}.

signal seems to have an effect similar to spontaneous emission noise effect [Fig. 11e1–e4]. On the other hand, despite positive $\Delta = 10$ GHz, the injected laser spectrum has a single peak centered at a frequency lower than the unperturbed laser frequency. Furthermore, the frequency width at half maximum $\approx 10^{10}\,s^{-1}$ [Fig. 11e5–e7] is much larger than the unperturbed laser spectrum but much narrower than the external signal spectrum [12]. In the bifurcation diagram, the laser signal intensity exhibits erratic oscillations whose amplitude increases with the external signal intensity [Fig. 12d1]. This increase appears to be continuous except for one abrupt transition at ≈ 0.15 W/cm^2.

Clearly, external signal phase-fluctuations can cause significant changes on the level of frequency spectrum and bifurcation diagram. However, neither frequency spectrum nor bifurcation diagram can always provide conclusive information on the changes in the dynamics owing to the external signal phase-fluctuations.

This information is revealed from calculating Lyapunov exponents of the corresponding random attractors. The largest (red) and the sum of two largest (blue) Lyapunov exponents are plotted in the right column in Fig. 12. Fig. 12a recalls already discussed result for the pure coherent injection and serves as a reference for phase-fluctuating external signals. Weak phase-fluctuations wash out most of the small periodic windows within chaotic region, weaken the signatures of bifurcations of periodic orbits, but have negligible effect on the position and extent of the chaotic region (Fig. 12b). As D_ϕ/π reaches $10^{10}\,s^{-1}$, Lyapunov exponents show significant deviations from the pure coherent injection case (Fig. 12c): (i) there is no indication of bifurcations of periodic orbits, (ii) all the periodic windows within the chaotic region are replaced with chaos, and (iii) there are no open intervals of periodic dynamics characterized by zero largest Lyapunov exponent. With further increase in D_ϕ, we observe that chaotic region still exists (Fig. 12d) but it is significantly shifted to higher external signal intensities (Fig. 12e). Interestingly, the abrupt transition at $\sim 0.15\,W/cm^2$ visible in the noisy bifurcation diagram in Fig. 12e1 appears to coincide with the crossing through zero of the largest Lyapunov exponent (Fig. 12e2).

The strong sensitivity of instabilities and chaos to external signal phase-fluctuation is summarised in Fig. 13 with plots of the largest Lyapunov exponent versus D_ϕ/π for two values of the external signal intensity. In particular, no effect is found for $D_\phi/\pi < 10^8\,s^{-1}$. However, when $(D_\phi/\pi) \approx 10^8\,s^{-1}$, phase-fluctuations start to impact the induced dynamics and modify the largest Lyapunov exponent. Furthermore, at $(D_\phi/\pi) \approx 10^{11}\,s^{-1}$, the two curves in Fig. 13 indicate a dramatic change in the type of induced dynamics: a sharp disappearance of chaos at injection intensity of $0.15\,w/cm^2$ (blue) and a concurrent sharp appearance of chaos at injection intensity of $6.9\,w/cm^2$ (red). For $(D_\phi/\pi) \gtrsim 10^{12}\,s^{-1}$ no additional change is observed.

The phenomena uncovered here can be understood intuitively. If the time scale of the external-signal phase-fluctation $(D_\phi/\pi)^{-1}$ is much longer than the time scale of the transient dynamics of the laser, the laser signal adiabatically follows any external-signal fluctuations. Consequently, the dynamics of the deterministic system is preserved and the net result of slow phase fluctuation is fluctuation in the laser signal and a smearing of the bifurcation boundaries. However, as $(D_\phi/\pi)^{-1}$ approaches the time scale of the transient dynamics of the laser, random phase fluctuations [Eq. (4)] and dynamics of a noise-free laser [Eqs. (1) and (2)] can no longer be separated. Rather, the two are strongly nonlinearly coupled giving rise to significant changes in the observed dynamics. The data in Fig. 13 shows two separate effects. Small changes to the largest Lyapunov exponent appear in the range $10^8\,s^{-1} \lesssim D_\phi/\pi \lesssim 10^{10}\,s^{-1}$ and an abrupt change takes place at $D_\phi/\pi \approx 10^{11}\,s^{-1}$. This result is a consequence of the two timescales underlying semiconductor laser dynamics: a slower one associated with the carrier decay rate $\gamma_N = 10^9\,s^{-1}$, and a faster one associated with the field decay rate $\gamma_c/2 = 5 \times 10^{11}\,s^{-1}$ (Table 1). Furthermore, mixing of the field and carrier time scales gives rise to relaxation oscillations and the red curve in Fig. 13 shows intermediate features when $(D_\phi/\pi)^{-1}$ becomes comparable to the relaxation oscillation timescale. For $(D_\phi/\pi)^{-1}$ much shorter than the time scale of the transient dynamics of the laser, phase fluctuations and dynamics of a noise-free laser can again be separated such that the laser signal experiences an average effect of the quickly-fluctuating external signal. More precisely, laser response is expected to equal the linear superposition of responses to a pure coherent signal [12]. Moreover, optical resonator acts as a filter with a Lorentzian lineshape and frequency width at half maximum equal to γ_c. Hence, no more changes appear in Fig. 13 for $D_\phi/\pi \gtrsim \gamma_c = 10^{12}\,s^{-1}$.

4.2.2. Amplitude noise

The product $\tau_c^{-1}D_\kappa$ gives the variance of the external signal amplitude-fluctuations about the mean value of the amplitude in the units of the mean value of the amplitude. Effects of different correlation time τ_c on different types of dynamics are shown in Fig. 14. If the external signal comes from another semiconductor laser, τ_c is typically much shorter than the time scale of the transient dynamics of the laser. In this case ($\tau_c = 10^{-12}\,s$), amplitude fluctuations have no effect on the chaotic dynamics (solid blue). For periodic oscillation (solid red) one observes a small decrease

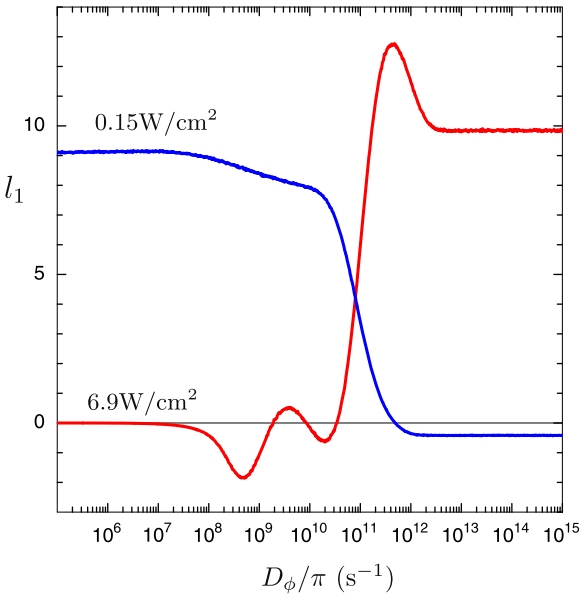

Fig. 13. The largest Lyapunov exponent in an optically injected Laser A vs. the rate of the external signal phase-fluctuations for two fixed values of the external signal intensity: (blue) 0.15 W/ cm^2 and (red) 6.9 W/cm^2 (K = (blue)15.5 and (red)105). Δ = 10 GHz and Λ_n = 2.

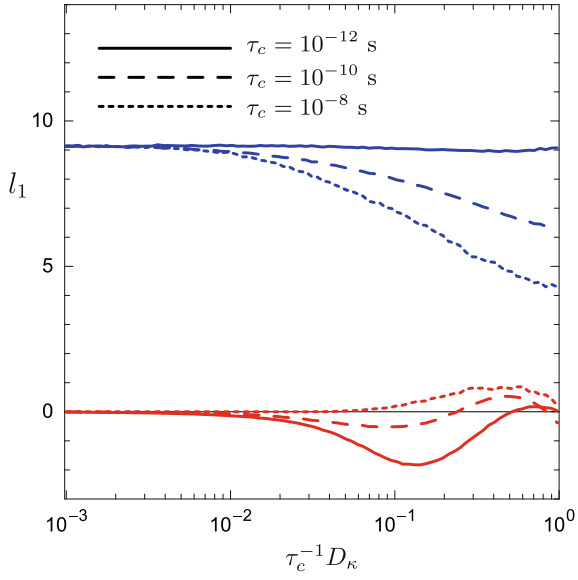

Fig. 14. The largest Lyapunov exponent in an optically injected Laser A vs. the strength of the external signal amplitude-fluctuations for two fixed values of the average external signal intensity: (three upper curves, blue) 0.15 W/cm^2 and (three lower curves, red) 6.9 W/cm^2(K = (three upper curves, blue) 15.5 and (three lower curves, red)105). The three different types of curves correspond to different values of the external signal correlation time: (solid) 10^{-12} s, (dashed) 10^{-10} s, and (dotted) 10^{-8} s. Δ = 10 GHz and Λ_n = 2.

in the maximum Lyapunov exponent from zero to negative values which is typical for limit-cycle oscillators driven by external noise [1]. Strong external signal amplitude-fluctuation can have noticeable effect on chaotic dynamics but this requires correlation time that is comparable to or much longer than the time scale of the transient dynamics of the laser. Specifically, the dashed and dotted blue curves show a noticeable decrease in the largest positive Lyapunov exponent for $\tau_c = 10^{-10}$ s and 10^{-8} s, respectively. An opposite effect of a long correlation time is observed on periodic dynamics. Specifically, dashed and dotted red curves show a small shift in the maximum Lyapunov exponent from zero to positive values. The observed shifts are due to "slow" amplitude fluctuation across the range of values which give rise to various dynamics including chaos and stable phase locking. Mixing of different responses to slowly fluctuating amplitude results on average in a decrease (increase) of the otherwise positive (negative) largest Lyapunov exponent. In overall, comparison between Figs. 13 and 14 shows that changes to the dynamics due to external signal amplitude-fluctuation are less significant than those due to phase-fluctuation.

5. Conclusions

This work investigates deterministic and stochastic versions of the rate equation model for an optically injected laser. The systematic analysis encompassing bifurcation diagrams, frequency spectra, and Lyapunov exponents, quantifies noise effects on the full range of externally induced laser dynamics and expands on the understanding of a general problem of dynamical sensitivity and nonlinear laser response. In particular, it uncovers and explains new phenomena owing to laser design and noise. While these studies are of fundamental interest regarding instabilities in nonlinear oscillators driven by noisy external signals, they also directly motivate laser sensor applications.

Our computations indicate drastic differences in the response of lasers with the same linewidth enhancement factor but different active-medium and optical-resonator parameters. Three quantities were identified as impacting the demonstrated difference in the nonlinear laser response, which are analytically known functions of transparency carrier density, differential gain coefficient, confinement factor, background refractive index, optical-resonator decay rate, and the pump rate. (1) Relaxation oscillation damping rate in an unperturbed laser determines the complexity of the externally induced instabilities and the normalised injection strength K at which instabilities occur. (2) Relaxation oscillation frequency of an unperturbed laser determines the frequency extent of the induced instabilities. (3) As the instability threshold is given by the normalised injection strength K, the optical-resonator design, or more precisely the external signal coupling-rate $c\sqrt{T}/[2n_bL\sqrt{(1-T)}]$, determines the external signal intensity required to induce the desired dynamics. The role of these three quantities is complementary to the role of the fourth quantity, the linedwidth enhancement factor, and the four quantities characterise the dynamical sensitivity of lasers to external optical signals. Maximum dynamical sensitivity in lasers is achieved for the combination of a large linewidth enhancement factor, small relaxation oscillation damping rate, large relaxation oscillation frequency, and optical-resonator parameters with largest $c\sqrt{T}/[2n_bL(\sqrt{(1-T)})]$. While the problem is illustrated using the example of an optically injected laser, the analysis applies to other laser systems too. Stabilising effects of the large relaxation–oscillation damping-rate have been observed in quantum-dot lasers with external optical feedback [41] and in coupled-cavity lasers [9].

The computations also demonstrated that externally induced instabilities and chaos can be significantly affected by spontaneous emission noise. Parameter regions, where strong spontaneous emission noise influence was expected, were identified using the relative noise strength. In particular, the mathematically interesting bifurcations found near the lasing threshold of the noise-free laser turn out not to be of physical relevance as they are typically washed out completely by the spontaneous emission noise. Furthermore, near the lasing threshold, spontaneous emission noise can cause a significant increase in the extent of the chaotic region (noise-induced chaos).

Our analysis uncovered new and interesting effects of external signal phase-fluctuation on the induced instabilities. Dynamics of the noise-free injected laser are unaffected by an external signal whose phase-fluctuations are much slower than the timescale of the transient dynamics of the laser, as the laser simply follows the slow changes in the external signal. When the timescale of the external signal phase-fluctuation becomes comparable with the timescale of the transient dynamics of the laser, drastic changes occur in the induced instabilities and chaos. Although particular bifurcations are washed out completely, the chaotic region remains but is shifted towards higher external signal intensities. Effects of external signal amplitude-fluctuation on laser instabilities are smaller than effects of phase-fluctuation and become noticeable only for strong fluctuations with the correlation time that is at least comparable to the time scale of the transient dynamics of the laser.

Finally, our results indicate that semiconductor lasers have strong potential for instability- and chaos-based remote sensing applications. The idea and procedure describing instability-based detection of weak coherent signals in the presence of strong incoherent background radiation is discussed in a different publication [42].

S.W. would like thank F. Kwasniok and R. Roy for stimulating discussions. The work of W.W.C. is supported in part by the US Department of Energy under contract DE–AC04–94AL8500 and the Alexander von Humboldt Foundation.

References

[1] A. Uchida, R. McAllister, R. Roy, Phys. Rev. Lett. 93 (2004) 244102.
[2] B. Krauskopf, D. Lenstra (Eds.), Fundamental Issues of Nonlinear Laser Dynamics, AIP Conference Proceedings, vol. 548, 2000.
[3] D.M. Kane, K.A. Shore (Eds.), Unlocking Dynamical Diversity: Optical Feedback Effects on Semiconductor Lasers, Wiley, 2005, p. 147.
[4] S. Wieczorek, B. Krauskopf, T.B. Simpson, D. Lenstra, Phys. Rep. 416 (2005) 1.
[5] C.H. Henry, IEEE J. Quantum Electron. QE-18 (1982) 259.
[6] S. Wieczorek, B. Krauskopf, D. Lenstra, Opt. Commun. 4172 (1–6) (1999) 279.
[7] S.K. Hwang, J.M. Liu, Opt. Commun. 183 (2000) 195.
[8] K.E. Chlouverakis, M.J. Adams, Opt. Commun. 216 (1) (2003) 405.
[9] S. Wieczorek, W.W. Chow, Opt. Commun. 246 (2005) 471.
[10] C. Mayol, R. Toral, C.R. Mirasso, M.A. Natiello, Phys. Rev. A 66 (2002) 013808.
[11] G. Vemuri, R. Roy, Opt. Commun. 77 (1990) 318.
[12] W.A. van der Graaf, A.M. Levine, D. Lenstra, IEEE J. Quantum Electron. 33 (1997) 434.
[13] M. Yousefi, D. Lenstra, G. Vemuri, Phys. Rev. E 67 (2003) 046213.
[14] G. Vemuri, R. Roy, Phys. Rev. A 39 (1989) 2539.
[15] I. Littler, S. Balle, K. Bergmann, G. Vemuri, R. Roy, Phys. Rev. A 41 (1990) 4131.
[16] E. Lacot, R. Day, F. Stoeckel, Phys. Rev. A 64 (2001) 043815.
[17] E. Lacot, O. Hugon, F. Stoeckel, Phys. Rev. A 67 (2003) 053806.
[18] F.T. Arecchi, R. Meucci, G. Puccioni, J. Tredicce, Opt. Commun. 51 (1984) 308.
[19] R. Lang, 'IEEE J. Quantum Electron. 18 (1982) 976.
[20] N. Shunk, K. Peterman, IEEE J. Quantum Electron. 22 (1986) 642.
[21] S. Wieczorek, W.W. Chow, L. Chrostowski, C.J. Chang-Hasnain, IEEE J. Quantum Electron. 42 (2006) 552.
[23] K. Vahala, A. Yariv, IEEE J. Quantum Electron. 19 (1983) 1102.
[24] C.H. Henry, IEEE J. Quantum Electron. 19 (1983) 1391.
[25] D.S. Elliot, S.J. Smith, J. Opt. Soc. Am. B5 (1988) 1927.
[26] F. Kéfélian, P. Gallion, IEEE J. Quantum Electron. 44 (2008) 547.
[27] E. Doedel, A. Champneys, T. Fairgrieve, Yu. Kuznetsov, B. Sandstede, X. Wang, <http://sourceforge.net/projects/auto2000/>.
[28] S. Wieczorek, T.B. Simpson, B. Krauskopf, D. Lenstra, Phys. Rev. E 65 (2002) 045207. R.
[29] S. Eriksson, Opt. Commun. 210 (2002) 343.
[30] S. Wieczorek, T.B. Simpson, B. Krauskopf, D. Lenstra, Opt. Commun. 215 (2003) 125.
[31] S. Valling, T. Fordell, A.M. Lindberg, Phys. Rev. A 72 (2005) 033810.

[33] M. Nizette, T. Erneux, A. Gavrielides, V. Kovanis, Proc. SPIE 3625 (1999) 679.
[34] G.H.M. van Tartwijk, G. Muijres, D. Lenstra, M.P. van Exter, J.P. Woerdman, IEEE J. Quantum Electron. 30 (1994) 1763.
[35] S.K. Hwang, J.B. Gao, J.M. Liu, Phys. Rev. E 61 (2000) 5162.
[37] L. Arnold, Random Dynamical Systems, Springer-Verlag, Berlin Heidelberg, 1998.
[38] M.T. Rosenstein, J.J. Collins, C.J. deLuca, Physica D 65 (1993) 117.
[39] H. Kantz, Phys. Lett. A 185 (1994) 77.
[40] J.P. Crutchfield, J.D. Farmer, B.A. Hubermann, Phys. Rep. 92 (1982) 45.
[41] D. O'Brian, S.P. Hegarty, G. Huyet, A.V. Uskov, Opt. Lett. 29 (2004) 1072.
[42] W.W. Chow, S. Wieczorek, Using chaos for remote sensing of laser radiation, Opt. Express, in press.